Am J Physiol Heart Circ Physiol 287: H937–H945, 2004;
10.1152/ajpheart.00877.2003.

Loss of PKC-δ alters cardiac metabolism

Manuel Mayr,[1] Yuen-Li Chung,[2] Ursula Mayr,[1] Emma McGregor,[5] Helen Troy,[2] Gottfried Baier,[3] Michael Leitges,[4] Michael J. Dunn,[6] John R. Griffiths,[2] and Qingbo Xu[1]

[1]*Department of Cardiac and Vascular Sciences and* [2]*Department of Basic Medical Sciences, St. George's Hospital Medical School, London SW17 0RE, United Kingdom;* [3]*Institute of Medical Biology and Human Genetics, University of Innsbruck, Innsbruck 6020, Austria;* [4]*Max-Planck-Institute for Experimental Endocrinology, Hannover 30625, Germany; and* [5]*Proteome Sciences and* [6]*Institute of Psychiatry, King's College, London SE5 8AF, United Kingdom*

Submitted 11 September 2003; accepted in final form 15 January 2004

Mayr, Manuel, Yuen-Li Chung, Ursula Mayr, Emma McGregor, Helen Troy, Gottfried Baier, Michael Leitges, Michael J. Dunn, John R. Griffiths, and Qingbo Xu. Loss of PKC-δ alters cardiac metabolism. *Am J Physiol Heart Circ Physiol* 287: H937–H945, 2004; 10.1152/ajpheart.00877.2003.—PKC-δ is believed to play an essential role in cardiomyocyte growth. In the present study, we investigated the effect of PKC-δ on cardiac metabolism using PKC-δ knockout mice generated in our laboratories. Proteomic analysis of heart protein extracts revealed profound changes in enzymes related to energy metabolism: certain isoforms of glycolytic enzymes, e.g., lactate dehydrogenase and pyruvate kinase, were absent or decreased, whereas several enzymes involved in lipid metabolism, e.g., phosphorylated isoforms of acyl-CoA dehydrogenases, showed a marked increase in PKC-$\delta^{-/-}$ hearts. Moreover, PKC-δ deficiency was associated with changes in antioxidants, namely, 1-Cys peroxiredoxin and selenium-binding protein 1, and posttranslational modifications of chaperones involved in cytoskeleton regulation, such as heat shock protein (HSP)20, HSP27, and the ζ-subunit of the cytosolic chaperone containing the T-complex polypeptide 1. High-resolution NMR analysis of cardiac metabolites confirmed a significant decrease in the ratio of glycolytic end products (alanine + lactate) to end products of lipid metabolism (acetate) in PKC-$\delta^{-/-}$ hearts. Taken together, our data demonstrate that loss of PKC-δ causes a shift from glucose to lipid metabolism in murine hearts, and we provide a detailed description of the enzymatic changes on a proteomic level. The consequences of these metabolic alterations on sensitivity to myocardial ischemia are further explored in the accompanying paper (20).

protein kinase C; proteomics; nuclear magnetic resonance; mouse model; metabolomics

PKC IS A HETEROGENEOUS FAMILY of phospholipid-dependent kinases that can be divided into three categories on the basis of cofactor requirements and structure: classical or conventional PKCs (α, β, and γ), novel PKCs (δ, ϵ, η, and θ), and atypical PKCs (ζ and ι) (25). Novel PKC isoforms are maximally activated by diacylglycerol in the absence of calcium, and recent evidence suggests a cross-regulation of novel PKC isoforms in cardiomyocytes (29). PKC-δ and PKC-ϵ are among the predominant isoforms of PKC in cardiac ventricles and have been implicated in heart failure, myocardial hypertrophy, and ischemic preconditioning (6, 9, 16).

Most of our knowledge about the role of PKC is derived from studies using a variety of inhibitors, many of which are not isoform specific and inhibit, to varying degrees, other protein kinases. Notably, the specificity of rottlerin, a widely used PKC-δ inhibitor, has recently been questioned (32): rottlerin appears to block PKC-δ activity indirectly in vivo by uncoupling mitochondria. Additionally, PKC isoform translocation is considered a hallmark of PKC activation. PKC-δ, however, is most efficiently tyrosine-phosphorylated among the PKC family, and phosphorylation is required for optimal PKC-δ activation in cardiomyocytes (10). Importantly, tyrosine phosphorylation and activation of PKC-δ without translocation has been observed after hydrogen peroxide stimulation (26). This finding suggests that translocation is an imperfect surrogate marker for PKC-δ activation and raises questions as to whether inhibition of PKC-δ translocation results in complete inhibition of PKC-δ-specific effects. Therefore, previous studies, especially on the PKC-δ isoform, have to be interpreted with caution.

To study the role of PKC-δ in cardiac tissues without using isozyme-nonselective chemical compounds or translocation inhibitors, we have recently created the first knockout mice lacking PKC-δ (11). We now combine the advantages of gene targeting and proteomic and metabolomic analysis to clarify the functional consequences of mutational ablation of the PKC-δ gene in cardiac tissues. By comparing the protein and metabolite profiles of wild-type and knockout hearts, we demonstrate PKC-δ-associated alterations in the proteome and provide firm evidence that hearts lacking PKC-δ show a metabolic shift from glycolysis toward increased fatty acid oxidation.

EXPERIMENTAL PROCEDURES

Mice and measurement of physiological parameters. All procedures were performed according to protocols approved by the Institutional Committee for Use and Care of Laboratory Animals. PKC-δ-deficient (PKC-$\delta^{-/-}$) mice were generated by targeted disruption of the endogenous PKC-δ gene. Genotypic characterization of adult mice by Southern blot analysis of genomic DNA indicated the successfully mutated allele (11). Systolic blood pressure and heart rate were measured using a noninvasive computerized tail-cuff system (BP-2000, Harvard Instruments). Mice were trained for 7 days by measuring blood pressure daily, after which blood pressure and heart rate were measured and recorded for 5 consecutive days. Additionally, blood pressure measurements were obtained by cannulating the carotid artery: mice underwent light anesthesia with thiopental (40 mg/kg im) followed by insertion of polyethylene catheters via the common carotid artery (34). The arterial catheter was connected to a pressure transducer (COBE; Lakewood, CO) and a blood pressure analyzer (Micro-MED; Louisville, KY). Measurements were recorded every 30 s for 10 min.

Address for reprint requests and other correspondence: Q. Xu, Dept. of Cardiac and Vascular Sciences, St. George's Hospital Medical School, Cranmer Terrace, London SW17 0RE, UK (E-mail: q.xu@sghms.ac.uk).

The costs of publication of this article were defrayed in part by the payment of page charges. The article must therefore be hereby marked "*advertisement*" in accordance with 18 U.S.C. Section 1734 solely to indicate this fact.

Proteomic analysis of heart tissue. Heart tissues for proteomic and metabolomic analysis were rinsed thoroughly with cold PBS to remove any blood components within the heart chambers, and whole hearts were frozen immediately in liquid nitrogen to avoid protein or metabolite degradation. The procedure used for proteomic analysis has been described previously (4, 21). Frozen heart samples were pulverized under liquid nitrogen into a fine powder. The resulting powder was homogenized in lysis buffer [containing 9.5 M urea, 2% (wt/vol) CHAPS, 0.8% (wt/vol) Pharmalyte pH 3–10, and 1% (wt/vol) DTT plus protease inhibitors] and centrifuged at 13,000 *g* at 20°C for 10 min. The supernatant was harvested, and protein concentration was determined. Solubilized samples were divided into aliquots and stored at −80°C. For two-dimensional (2-D) gel electrophoresis, extracts were loaded on nonlinear immobilized pH gradient (IPG) 18-cm strips (3–10, Amersham Pharmacia Biotech). For analytic and preparative gels, respectively, a protein load of 100 and 400 μg was applied to each IPG strip using an in-gel rehydration method. Samples were diluted in rehydration solution [containing 8 M urea, 0.5% (wt/vol) CHAPS, 0.2% (wt/vol) DTT, and 0.2% (wt/vol) Pharmalyte pH 3–10] and rehydrated overnight in a reswelling tray. Strips were focused at 0.05 mA/IPG strip for 60 kV·h at 20°C. Once isoelectric focusing was completed, the strips were equilibrated in 6 M urea containing 30% (vol/vol) glycerol, 2% (wt/vol) SDS, and 0.01% (wt/vol) bromphenol blue with the addition of 1% (wt/vol) DTT for 15 min, followed by the same buffer without DTT but with the addition of 4.8% (wt/vol) iodoacetamide for 15 min. SDS-PAGE was performed using 12% T, 2.6% C separating polyacrylamide gels without a stacking gel, using the Hoefer DALT system. The second dimension was carried out overnight at 20 mA/gel at 8°C and was terminated when the bromphenol dye front had migrated off the lower end to the gels. After electrophoresis, gels were fixed for a minimum of 1 h in methanol-acetic acid-water solution [4:1:5 (vol/vol/vol)]. 2-D gel electrophoresis protein profiles were visualized in preparative gels by silver staining using the Plus One silver staining kit (Amersham Pharmacia Biotech) with slight modifications to ensure compatibility with subsequent mass spectroscopy (MS) analysis (35). Analytic gels were stained with a more sensitive silver staining kit (Owl, UK). For the detection of phosphoproteins, 2-D electrophoresis gels were stained with Pro-Q Diamond (Molecular Probes) according to the manufacturer's instruction and scanned on a Typhoon 9400 scanner (Amersham Biosciences) at 532 nm, with the emission filter set at 560 LP and the photomultiplier tube set at 600 V. Counterstaining was performed with Sypro Ruby (Molecular Probes). Spot patterns were analyzed using Progenesis (Nonlinear Dynamics), Proteomweaver (Definiens), and PDQuest software (Bio-Rad). Spots showing a statistical difference in intensity were excised for identification.

Mass spectrometry. Gel pieces containing selected protein spots were treated overnight with modified trypsin (Promega) according to a previously published protocol (31). Peptide fragments were recovered by sequential extractions with 50 mM ammonium hydrogen carbonate, 5% (vol/vol) formic acid, and acetonitrile 50% (vol/vol). Extracts were lyophilized, resuspended in 20 μl of 0.1% (vol/vol) trifluoroacetic acid-10% (vol/vol) acetonitrile, and desalted on Millipore Zip tips according to the manufacturer's instructions. Matrix-assisted laser desorption/ionization-MS was performed using an Axima CFR spectrometer (Kratos; Manchester, UK). The instrument was operated in the positive ion reflectron mode. α-Cyano-4-hydroxycinnaminic acid was applied as the matrix. Spectra were internally calibrated using trypsin autolysis products. The resulting peptide masses were searched against databases using the MASCOT program (27). One missed cleavage per peptide was allowed, and carbamidomethylation of cysteine as well as partial oxidation of methionine were assumed. In addition to MALDI-MS, tandem MS was performed for the sequencing of tryptic digest peptides. After enzymatic degradation, peptides were separated by capillary liquid chromatography on a reverse-phase column (BioBasic-18, 100 × 0.18 mm, particle size 5 μm, Thermo Electron) and applied to a LCQ ion-trap mass spectrometer (LCQ Deca XP Plus, Thermo Finnigan). Spectra were collected from the ion-trap mass analyzer using full ion scan mode over the mass-to-charge (*m*/*z*) range of 300–2,000. MS-MS scans were performed on each ion using dynamic exclusion. A database search was performed using the TurboSEQUEST software (Thermo Finnigan).

RT-PCR. Total RNA from heart tissues was extracted using the Fast RNA kit according to the protocol provided by the manufacturer (Qiagen). Total RNA (2 μg) was reverse transcribed into cDNA using the Promega RT system. The RT products were examined by PCR with 1-Cys peroxiredoxin (1-Cys prx) primers producing 203-bp fragments (24) and GAPDH primers producing 309-bp fragments.

Western blotting. Western blotting was performed as described previously (13, 14). For immunoblotting of 2-D electrophoresis gels, 100 μg of protein were loaded on nonlinear IPG 7-cm strips (3–10, Amersham Pharmacia Biotech) by active rehydration (30 V, 12 h) and focused for 13 kV·h using the IPG phor system (Amersham Pharmacia Biotech). After being focused, the strips were equilibrated as described above, separated on 4–12% Tris-glycine zoom gels (Invitrogen), and blotted onto nitrocellulose membranes. Antibodies to the cytosolic chaperone containing the T-complex polypeptide (CCT) subunits were kindly provided by Dr. A. Roobol (University of Kent, Canterbury, UK).

Proton NMR spectroscopy. Snap-frozen hearts were extracted in 6% perchloric acid (1). Neutralized extracts were freeze dried and reconstituted in D_2O. Extracts (0.5 ml) were placed in 5-mm NMR tubes. ^{1}H NMR spectra were obtained using a Bruker 500-MHz spectrometer. The water resonance was suppressed by using gated irradiation centered on the water frequency. Sodium 3-trimethylsilyl-2,2,3,3-tetradeuteropropionate (TSP) was added to the samples for chemical shift calibration and quantification. Immediately before the NMR analysis, the pH was readjusted to 7 with PCA or KOH.

Statistical analysis. Statistical analysis was performed using ANOVA and Student's *t*-test, respectively. Results are given as means ± SD. A P value of <0.05 was considered significant.

RESULTS

Physiological characteristics. PKC-$\delta^{-/-}$ mice were indistinguishable from their wild-type littermates; they developed normally and were fertile. The null allele was confirmed by the absence of PKC-δ expression in a variety of tissues, including the heart (11). PKC-$\delta^{-/-}$ mice showed no overt cardiac phenotype and no significant differences in physiological variables, such as body weight, heart rate, and arterial blood pressure (measured by the cuff technique as well as by cannulating the carotid artery; Table 1). The heart weight-to-body weight ratio was slightly lower in PKC-$\delta^{-/-}$ mice; however, this difference failed to reach statistical significance ($P = 0.24$; Table 1).

Enzymatic changes in the proteome of PKC-$\delta^{-/-}$ hearts. To provide insights into the potential cellular targets of PKC-δ, we analyzed the changes in the proteome by 2-D gel electrophoresis. Average gels for PKC-$\delta^{+/+}$ and PKC-$\delta^{-/-}$ hearts were

Table 1. *Baseline parameters of PKCδ$^{+/+}$ and PKCδ$^{-/-}$ mice*

Parameters	PKCδ$^{+/+}$	PKCδ$^{-/-}$
n	11	8
Body weight, g	25.7±1.2	26.1±0.9
Heart weight-to-body weight ratio, %	0.48±0.015	0.45±0.022
Blood pressure, mmHg	110±5	118±3
Heart rate, beats/min	331±20	312±19

Values are means ± SE; *n*, no. of mice.

created from 4 gels/group. A direct overlay is presented in Fig. 1. With the use of a broad-range pH gradient (pH 3–10 nonlinear), 2-D electrophoresis gels compromised ~1,400 protein features. Differentially expressed spots were highlighted in color (orange and blue indicate an increase in PKC-$\delta^{+/+}$ and PKC-$\delta^{-/-}$ hearts, respectively; Fig. 1). Numbered spots were excised and subject to in-gel tryptic digestion. Protein identifications as obtained by MALDI-MS are listed in Table 2.

Strikingly, most of the changes observed in PKC-$\delta^{-/-}$ hearts were related to energy metabolism. Enzymes involved in glycolysis, e.g., isoforms of glycerol-3-phosphate dehydrogenase, pyruvate kinase, and lactate dehydrogenase, were less abundant compared with wild-type controls, whereas certain enzymatic species related to lipid metabolism were found to be markedly upregulated in PKC-$\delta^{-/-}$ hearts: a three- and five-fold increase was observed for two isoforms of acyl-CoA dehydrogenase, which are responsible for β-oxidation of short-chain fatty acids. However, their isoelectric points (pI) in 2-D electrophoresis gels were very different from the calculated one (Table 2), and subsequent staining for phosphoproteins demonstrated that these isoforms are highly phosphorylated (Fig. 2*A*). Similarly, propionyl-CoA carboxylase, an enzyme involved in fatty acid metabolism, appeared as a row of several spots with different pI and the same molecular mass in PKC-$\delta^{-/-}$ hearts (Fig. 1), indicating again altered posttranslational modifications rather than changes in protein expression. Concomitantly, aldehyde deydrogenase 4 family member A_1 and Ke 6 protein were found to be present in more acidic isoforms in PKC-$\delta^{-/-}$ hearts (Fig. 1). The acidic shift of aldehyde deydrogenase 4 family member A_1 in PKC-$\delta^{-/-}$ hearts was associated with the presence of a mitochondrial precursor sequence (Fig. 2*B*). Notably, this enzymatic precursor was not expressed at detectable levels in PKC-$\delta^{+/+}$ hearts. Taken together, our proteomic data suggest increased lipid metabolism in PKC-$\delta^{-/-}$ hearts.

Antioxidants in PKC-$\delta^{-/-}$ hearts. Another interesting observation in our proteomic analysis was the absence of the oxidized form of 1-Cys prx in PKC-$\delta^{-/-}$ hearts (Fig. 3*A*). Peroxiredoxins represent a special type of peroxidases as the protein is the reducing substrate itself; upon oxidative stress, the active site in 1-Cys prx is either oxidized to cysteine sulfenic acid or overoxidized to cysteine sulfonic acid. While the first modification is DTT sensitive and therefore undetectable in 2-D electrophoresis gels, the latter modification is DTT resistant and results in a charge shift toward a more acidic pI (33). Thus 1-Cys prxs are often encountered as doublet spots in 2-D electrophoresis. Interestingly, 1-Cys prx was exclusively present as a DTT sensitive (basic) isoform in PKC-$\delta^{-/-}$ hearts, whereas the predominant isoform in wild-type hearts was the DTT insensitive (acidic) one, corresponding to overoxidation of the active site cysteine into a cysteine sulfonic acid (Fig. 3*A*).

This overoxidation is likely to be irreversible under biological conditions, and de novo synthesis of 1-Cys prx is required

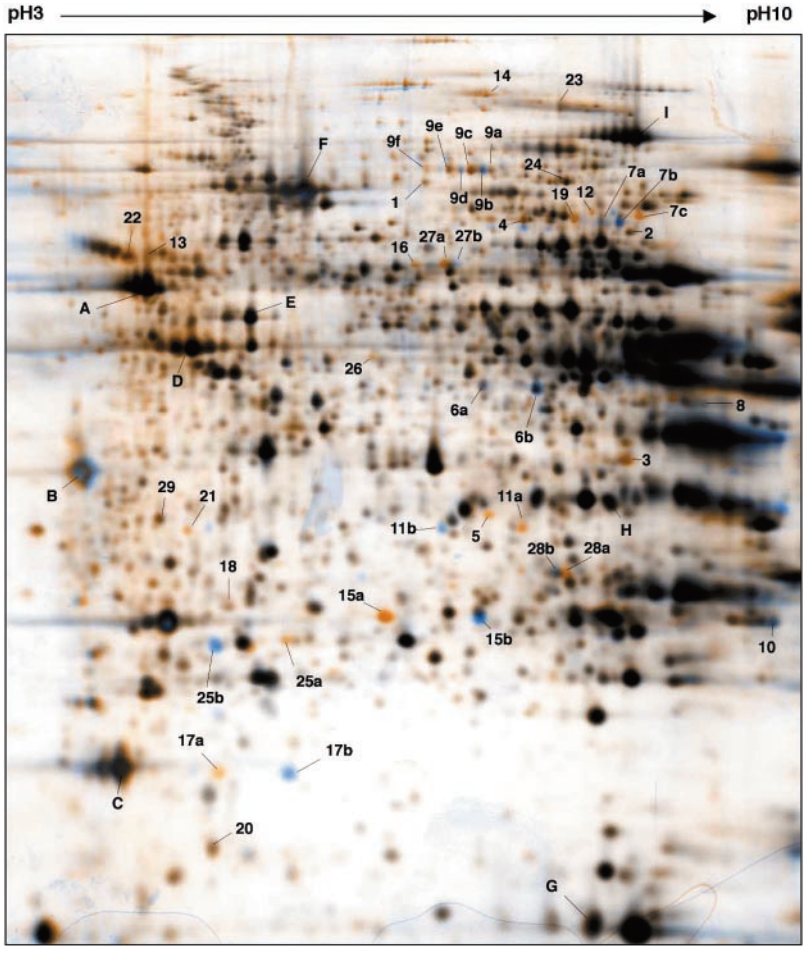

Fig. 1. Two-dimensional (2-D) electrophoresis map of heart proteins. Protein extracts were separated on a pH 3–10 nonlinear IPG strip, followed by a 12% SDS polyacrylamide gel. Spots were detected by silver staining. A direct overlay of average gels from PKC-$\delta^{+/+}$ and PKC-$\delta^{-/-}$ hearts is shown. Each average gel was created from 4 single gels (total $n = 8$). Differentially expressed spots are highlighted in color (orange and blue for PKC-$\delta^{+/+}$ and PKC-$\delta^{-/-}$ hearts, respectively). Proteins identified by MALDI-MS are marked with numbers and listed in Table 2. The following letters label proteins used as reference spots for molecular mass and isoelectric points (pI): ATP synthase β-subunit of the H^+-transporting mitochondrial F_1 complex (theoretical mass/pI: 56 kDa/5.2) (A); α-tropomyosin (theoretical mass/pI: 32.7 kDa/4.7) (B); myosin light chain-phosphorylatable cardiac ventricles (theoretical mass/pI: 18.9 kDa/4.9) (C); cardiac α-actin (theoretical mass/pI: 41.8 kDa/5.3) (D); core protein 1 of ubiquinol-cytochrome *c* reductase (theoretical mass/pI: 52.7 kDa/5.8) (E); serum albumin (theoretical mass/pI: 68.8 kDa/5.8) (F); myoglobin (theoretical mass/pI: 17.1 kDa/7.1) (G); voltage-dependent anion channel 2 (theoretical mass/pI: 31.7 kDa/7.4) (H); and mitochondrial aconitase 2 (theoretical mass/pI: 85.4 kDa/8.1) (I).

Table 2. *Differences in protein profiles between hearts of PKCδ$^{+/+}$ and PKCδ$^{-/-}$ mice*

Spot Number	Protein identity	Δ	*P* Value	NCBI Entry Number	Function	Calculated pI/ Mol. Mass, Da ($\times 10^3$)	Observed pI/ Mol. Mass, Da ($\times 10^3$)	Sequence Coverage/ Mascot Score
					Glucose metabolism			
1	Glycerol-3-phosphate dehydrogenase	−2.2	0.011	31981769	Glycolysis	6.2/81.4	5.9/70.2	14%/90
2	Pyruvate kinase 3	−2.0	0.007	20890302	Final step in glycolysis	6.7/57.9	8.0/58.7	16%/100
3	Lactate dehydrogenase 1	−3.5	0.001	13529599	Anaerobic glycolysis	8.2/34.5	7.9/34.3	32%/107
4	Riken cDNA 2610207(Δi)16	−2.5	0.012	13195670	Glucose/ribitol dehydrogenase	6.3/54.9	6.1/59.4	14%/91
5	Mercaptopyruvate sulfurtransferase	WT	0.000	20149758	Conversion of cysteine to pyruvate	6.1/33.0	6.0/32.2	36%/113
					Lipid metabolism			
6a	Acyl-Coenzyme A dehydrogenase, short chain specific	+3.5	0.024	20841295	β-Oxidation of short-chain fatty acids	8.9/44.9	6.0/38.6	25%/110
6b	Acyl-coenzyme A dehydrogenase, short chain specific	+5.0	0.026	584714	β-Oxidation of short-chain fatty acids	9.0/44.9	6.3/38.6	15%/76
7a	Similar to aldehyde dehydrogenase 4 family member A_1, mitochondrial precursor	Null	0.025	24659695	Oxidation of aliphatic and aromatic aldehydes	8.7/63.2	7.8/62.0	14%/103
7b	Aldehyde dehydrogenase 4 family member A_1	+5.6	0.013	18848352	Oxidation of aliphatic and aromatic aldehydes	8.3/60.3	8.0/62.0	20%/87
7c	Aldehyde dehydrogenase 4 family member A_1	WT	0.002	18848352	Oxidation of aliphatic and aromatic aldehydes	8.3/60.3	8.1/62.0	14%/80
8	Peciprotein	+6.7	0.005	12805053	Peroxisomal enoyl-CoA isomerase	8.1/39.4	8.5/38.0	21%/125
9a	Propionyl-CoA carboxylase, α-subunit	−3.5	0.003	21450241	β-Oxidation of odd-chain fatty acids	7.0/79.9	6.0/73.1	12%/97
9b	Propionyl-CoA carboxylase α-subunit	Null	0.016	21450241	β-Oxidation of odd-chain fatty acids	7.0/79.9	6.0/73.4	17%/111
9c	Propionyl-CoA carboxylase α-subunit	−3.5	0.004	21450241	β-Oxidation of odd-chain fatty acids	7.0/79.9	6.0/73.8	10%/84
9d	Propionyl-CoA carboxylase α-subunit	Null	0.008	21450241	β-Oxidation of odd-chain fatty acids	7.0/79.9	5.9/73.9	16%/93
9e	Propionyl-CoA carboxylase α-subunit	−4.0	0.001	21450241	β-Oxidation of odd-chain fatty acids	7.0/79.9	5.9/73.9	29%/152
9f	Propionyl-CoA carboxylase α-subunit	−4.8	0.000	21450241	β-Oxidation of odd-chain fatty acids	7.0/79.9	5.8/73.9	16%/73
10	3-Hydroxyacyl-CoA dehydrogenase type II	+4.3	0.045	7949047	short-chain/hydroxy-steroid dehydrogenase	8.8/27.4	9.5/24.6	36%/96
11a	Ke 6 protein	WT	0.010	1103844	Alcohol/steroid dehydrogenase	6.1/26.7	6.1/27.0	38%/143
11b	Ke 6 protein	Null	0.010	1103844	Alcohol/steroid dehydrogenase	6.1/26.7	5.9/27.0	44%/172
12	Malic enzyme, supernatant	WT	0.000	6678912	NADPH generation	7.2/63.9	7.1/63.0	9%/63
					Respiratory chain/TCA cycle			
13	ATP synthase, H^+ transporting mitochondrial F1 complex, β-subunit	−6.8	0.001	12832739	ATP generation, respiratory chain	5.4/56.9	5.0/57.4	37%/200
14	Oxoglutarate dehydrogenase (lipoamide, E_1 component)	−3.5	0.001	20853413	TCA cycle	6.4/116.4	5.9/110.3	19%/148
					Antioxidants			
15a	1-Cys peroxiredoxin (antioxidant protein 2)	WT	0.004	6671549	Nonselenium glutathione peroxidase	6.0/24.8	5.9/24.8	22%/90
15b	1-Cys peroxiredoxin (antioxidant protein 2)	+3.0	0.000	6671549	Nonselenium glutathione peroxidase	6.0/24.8	6.0/24.8	50%/188
16	Selenium-binding protein 1	−7.5	0.000	134259	Intracellular selenium transport	6.0/52.3	5.9/52.8	16%/77
					Chaperones			
17a	Similar to HSP20	WT	0.025	20825064	Actin binding	5.6/17.5	5.3/18.3	26%/90
17b	Similar to HSP20	Null	0.023	20825064	Actin binding	5.6/17.5	5.6/17.5	29%/69
18	HSP27	−4.2	0.010	7305173	Actin regulation	6.4/22.9	5.4/25.2	36%/103
19	Chaperonin containing TCP-1 subunit 6a (ζ)	Null	0.000	6753324	Tubulin folding	6.6/58.0	6.8/61.5	19%/89
					Others			
20	Atrial natriuretic factor precursor	−2.7	0.029	113865	Vasodilatative peptide	6.7/16.6	5.3/15.9	28%/80
21	Similar to aurora A	WT	0.024	20821951	Protein kinase	5.8/33.1	5.2/30.3	17%/62
22	Spi1-4 protein	−5.5	0.003	15929675	Splice isoform of α_1-antitrypsin	5.3/45.6	4.9/56.4	30%/109
23	Oracle2 protein	−3.5	0.012	6969631	Cypher 1	8.3/70.7	7.2/90.4	22%/141
24	Mitofilin	−2.7	0.005	29427692	Heart mitochondrial inner membrane protein	6.2/83.8	6.7/70.3	37%/214
25a	Apolipoprotein A-I	WT	0.023	6753096	Reverse cholesterol transport	5.4/30.4	5.6/23.7	27%/102
25b	Apolipoprotein A-I	+4.3	0.024	6753096	Reverse cholesterol transport	5.4/30.4	5.3/23.5	40%/155
26	Methyltransferase CYT 19	WT	0.023	15488645	Methylation of arsenic	5.8/41.8	5.8/40.5	26%/87
27a	Similar to hypothetical protein FLJ10759	WT	0.000	20843813	SPRY domain-containing protein	6.0/52.8	5.9/52.8	38%/194
27b	Similar to hypothetical protein FLJ10759	Null	0.000	20843813	SPRY domain-containing protein	6.0/52.8	6.0/52.8	33%/105
28a	Unknown (protein for MGC:62540)	WT	0.004	33243954	Splice isoform of carbonic anhydrase 2	6.5/29.0	6.7/26.3	33%/120
28b	Unknown (protein for MGC:62540)	+3.5	0.001	33243954	Splice isoform of carbonic anhydrase 2	6.5/29.0	6.6/26.3	30%/104
29	Riken cDNA 2310005O14	−2.2	0.011	20885971	Unknown function	5.6/35.1	5.0/32.4	30%/120

Δ, Fold increased/decreased expression in PKCδ$^{-/-}$ hearts compared with PKCδ$^{+/+}$ hearts; WT and Null indicate unique protein species of wild-type and PKC-δ null hearts. pI, isoelectric point; TCA, tricarboxylic acid; HSP, heat shock protein.

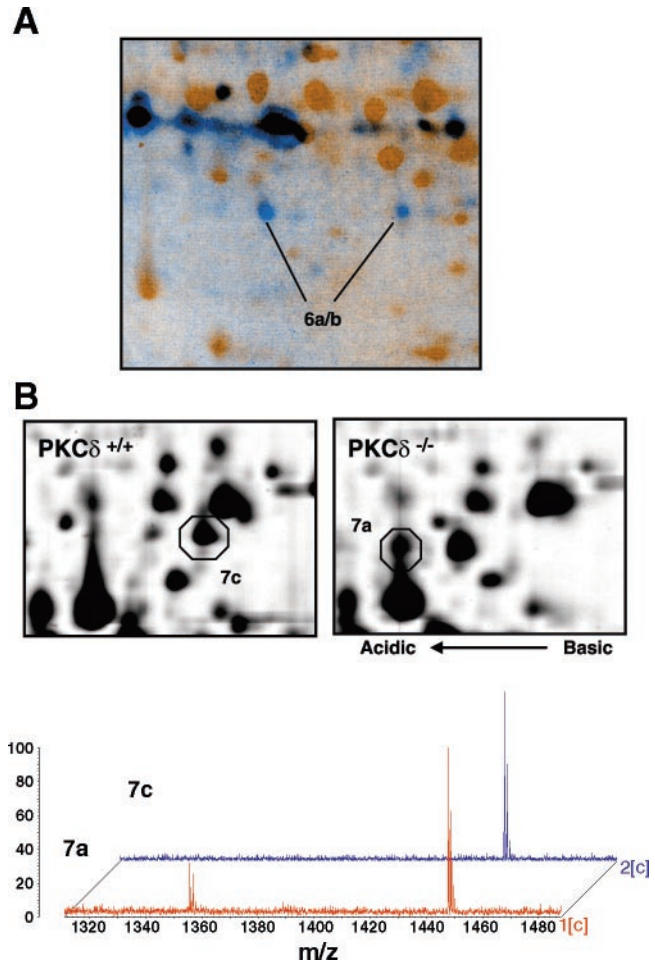

Fig. 2. Enzymes related to lipid metabolism in PKC-$\delta^{-/-}$ hearts. *A*: increased phosphorylation of acyl-CoA dehydrogenases in PKC-$\delta^{-/-}$ hearts. Numbers correspond to protein identities in Fig. 1. Phosphoproteins are highlighted in blue. Counterstaining was performed with Sypro ruby and is visualized in orange. *B, top*: presence of mitochondrial precursor proteins in PKC-$\delta^{-/-}$ hearts. *Spots 7a* and *7c* are highlighted on 2-D electrophoresis gels. Their corresponding mass spectrometry (MS) spectra are also shown (*bottom*). The peptide at 1,355.82 kDa in the spectrum of *spot 7a* matches to amino acid residues 7–18 in the mitochondrial precursor sequence of aldehyde dehydrogenase 4 family member A_1. This precursor peptide is absent in the spectrum of *spot 7c*, the predominant isoform of aldehyde dehydrogenase 4 family member A_1 in PKC-$\delta^{+/+}$ hearts. *m/z*, Mass-to-charge ratio.

to counteract the annihilation of the peroxiredoxin-based antioxidant defence (28). Consistent with the predominance of the acidic isoform in PKC-$\delta^{-/-}$ hearts, RT-PCR showed higher levels of 1-Cys prx mRNA, indicating an increased turnover of this antioxidant protein compared with PKC-$\delta^{-/-}$ hearts (Fig. 3*B*). Total protein levels of 1-Cys prx were almost twofold decreased in PKC-$\delta^{-/-}$ hearts, as estimated by quantification on 2-D electrophoresis gels (Fig. 3*A*; signal intensity 4,055 vs. 2,179 arbitrary units). Similarly, expression of selenium-binding protein 1, another protein related to protection against oxidative stress, was altered in PKC-$\delta^{-/-}$ hearts (Table 2).

Changes in chaperones in PKC-$\delta^{-/-}$ hearts. Previous findings in PKC-δ transgenic mice demonstrated that inhibition of PKC-δ translocation resulted in focal cytoskeletal disruption and upregulation of crystallin-α/B (6), the most abundant small heat shock protein (HSP) in cardiac tissue. In PKC-$\delta^{-/-}$ hearts, no quantitative difference in crystallin-α/B expression was observed (Fig. 4*A*), but a protein similar to HSP 20 was found to be present in a more basic isoform compared with PKC-$\delta^{+/+}$ hearts (Fig. 4*B*, *spots 17a* and *17b*). Its identification was confirmed by tandem MS (Fig. 4*C*). A common modification causing such pI changes on 2-D gels is dephosphorylation: whereas phosphorylated HSP20 is proposed to interact with monomeric actin, dephosphorylated forms of HSP20 bind to polymeric actin. HSP20 may also form heterocomplexes with other HSPs, including crystallin-α/B.

Furthermore, HSP27 and the ζ-subunit of CCT-1 were differentially expressed in PKC-$\delta^{-/-}$ hearts (Table 2). Because no differences in protein abundance were observed in Western blots of one-dimensional gels (Fig. 5*A*), we verified our findings by immunoblotting of 2-D gels. HSP27 was visualized as a charge train consisting of three major spots (Fig. 5*B*), which are known to represent different phosphorylation states. The most acidic (and most phosphorylated) spot of HSP27 was less abundant in PKC-$\delta^{-/-}$ hearts (Fig. 5*B*, *bottom*). This is in excellent agreement with our findings in 2-D gels, where *spot 18* was identified as HSP27 with an estimated pI of 5.4 compared with the theoretical value of 6.4.

Although HSP27 is known to be efficiently phosphorylated by PKC-δ (18), there has been no evidence so far that PKC-δ plays a role in regulating CCT-1. CCT-1 is a heterooligomeric complex of eight different subunits. Its folding substrate specificity is mainly restricted to actin and tubulin, with the ζ-subunit being involved in tubulin binding (17). Immunoblotting of 2-D gels revealed that the most basic isoform of CCT-ζ was absent in PKC-$\delta^{-/-}$ hearts, whereas no differences were observed for other subunits (Fig. 5, *C* and *D*). Thus changes in 2-D gels represented no differences in protein abundance but reflected altered posttranslational modification.

Metabolic changes in PKC-$\delta^{-/-}$ hearts. Enzymatic changes constituted by far the majority of differences in the protein profile of PKC-$\delta^{-/-}$ hearts. To clarify the metabolic net effect of these proteomic changes, we measured cardiac metabolites with high-resolution NMR spectroscopy (Fig. 6) (5). Within the aliphatic region (−0.05 to 4.2 ppm) of the NMR spectra, resonances have been assigned to α-ketoisovalerate, lactate, alanine, acetate, glutamate, succinate, creatine, choline, carnitine, taurine, and glycine (5). The presence of glycerophosphocholine within the carnitine peak was ruled out by NMR analysis at low pH. NMR spectra of PKC-$\delta^{+/+}$ and PKC-$\delta^{-/-}$ hearts are shown in Fig. 6, *A* and *B*. Metabolite concentrations were similar in wild-type and knockout hearts except for the ratio of glycolytic end products (alanine + lactate) to end products of lipid metabolism (acetate), which was significantly decreased in PKC-$\delta^{-/-}$ hearts (Fig. 6*C*). Thus our metabolomic data confirm the functional relevance of the proteomic changes described above.

DISCUSSION

PKC-δ activation is thought to be crucial in cardiac pathology, such as cardiac hypertrophy, heart failure, and ischemia-reperfusion injury (6, 9, 16). Accordingly, delineating the in vivo effects of PKC-δ in myocardial tissue is a scientific priority. So far, approaches to study PKC-δ activation in hearts have included the use of isozyme-nonselective inhibitors. In the present study, we investigated the role of PKC-δ in cardiac

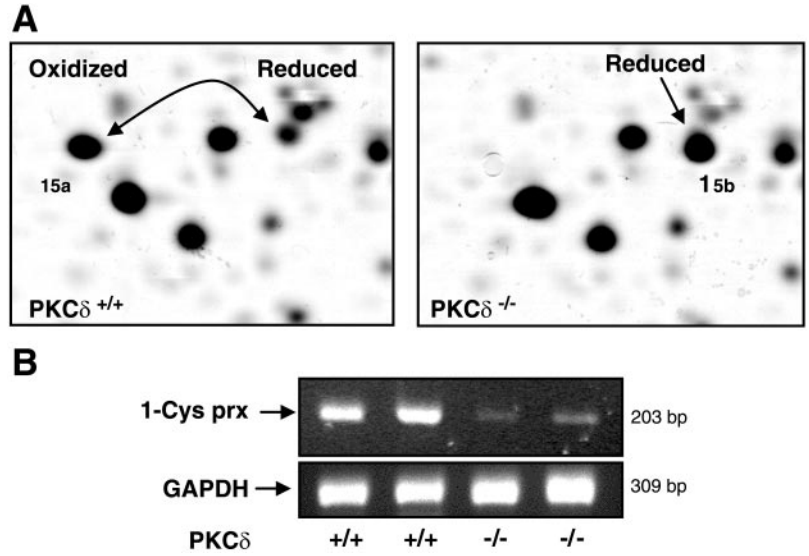

Fig. 3. Oxidative stress in PKC-$\delta^{-/-}$ hearts. The spot pair corresponding to 1-Cys peroxiredoxin (1-Cys-Prx) in PKC-$\delta^{+/+}$ hearts is marked with an arrow (*A*). Numbers correspond to protein identities in Fig. 1. Note the absence of the oxidized isoform in PKC-$\delta^{-/-}$ hearts. The expression of 1-Cys prx was examined by RT-PCR (*B*).

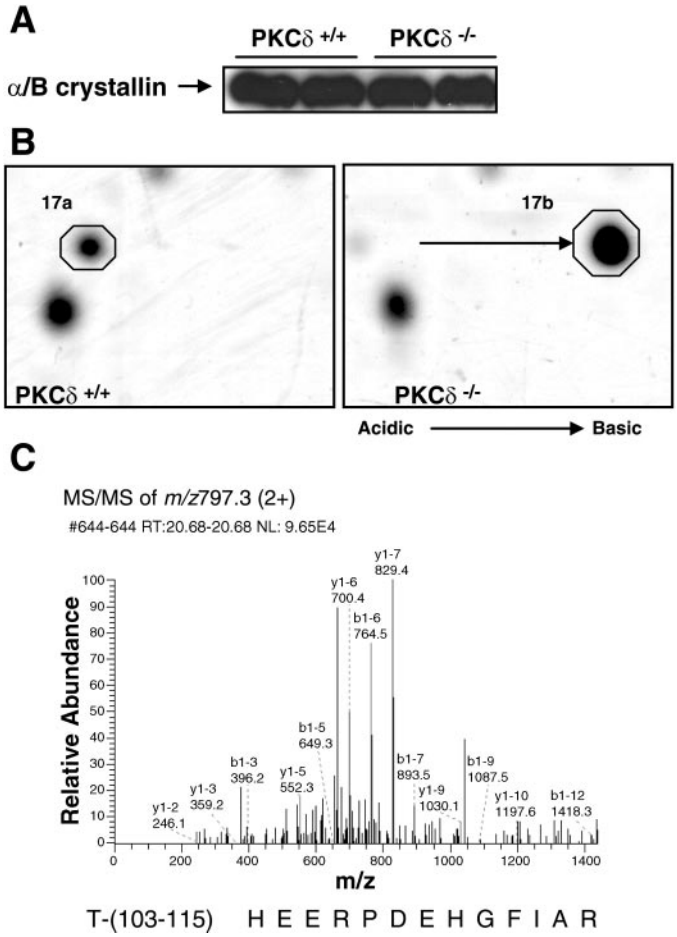

Fig. 4. Differential expression of heat shock protein (HSP)20 in PKC-$\delta^{-/-}$ hearts. *A*: Western blot analysis of crystallin α/β expression. *B*: changes in expression of HSP20 in PKC-$\delta^{+/+}$ and PKC-$\delta^{-/-}$ hearts. *C*: the product ion spectrum of the doubly charged tryptic peptide T-(103–115) at *m/z* 797.3 was identified as a protein "similar to HSP20": HEERPDEHGFIAR.

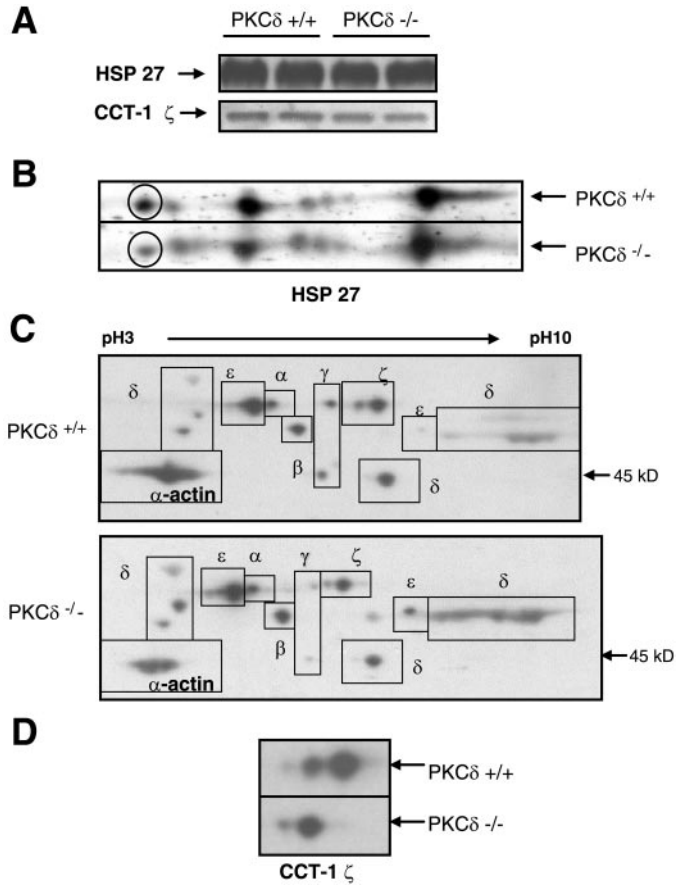

Fig. 5. HSP27 and cytosolic chaperone containing the T-complex polypeptide (CCT) subunit expression in PKC-$\delta^{-/-}$ hearts. *A*: quantification of protein abundance using one-dimensional SDS-PAGE. *B–D*: 2-D electrophoresis gels from PKC-$\delta^{+/+}$ and PKC-$\delta^{-/-}$ hearts were immunoanalyzed for HSP27 (*B*) and CCT subunits (*C* and *D*) as described in MATERIALS AND METHODS. *B* and *D* show a direct overlay of immunostained blots from PKC-$\delta^{+/+}$ and PKC-$\delta^{-/-}$ hearts, highlighting the differences in isoform expression.

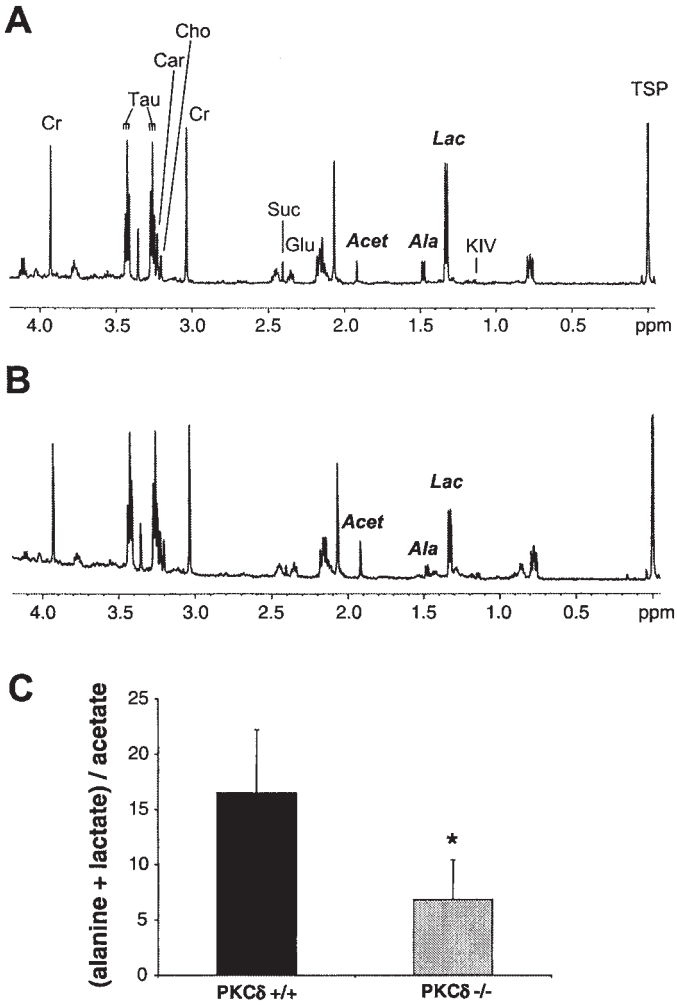

Fig. 6. *A* and *B*: NMR spectra of PKC-$\delta^{+/+}$ (*A*) and PKC-$\delta^{-/-}$ hearts (*B*). Resonances were assigned to α-ketoisovalerate (KIV), lactate (Lac), alanine (Ala), acetate (Acet), glutamate (Glu), succinate (Suc), creatine (Cr), choline (Cho), carnitine (Car), taurine (Tau), and glycine (Gly). Sodium 3-trimethylsilyl-2,2,3,3-tetradeuteropropionate (TSP) was added to the samples for calibration. *C*: ratio of (Ala + Lac) to (Acet) (n = 5 PKC-$\delta^{+/+}$ hearts and 3 PKC-$\delta^{-/-}$ hearts, *$P < 0.05$).

tissue by using PKC-δ knockout mice. Mutational ablation of the PKC-δ gene caused profound alterations in the proteome and metabolome, which resulted in a metabolic shift from glycolysis toward increased lipid metabolism. Considering the importance of energy metabolism in cardiac tissues, our findings could contribute to a better understanding of PKC-δ isoform specific effects in the pathological conditions mentioned above.

Altered energy generation in PKC-$\delta^{-/-}$ hearts. It has been demonstrated that PKC-δ and PKC-ϵ have overlapping functions in myocardial growth (3). This functional redundancy might explain why neither PKC-$\epsilon^{-/-}$ nor PKC-$\delta^{-/-}$ mice show an overt cardiac phenotype. However, expression levels of PKC-ϵ as studied by Western blot analysis were similar in PKC-$\delta^{+/+}$ and PKC-$\delta^{-/-}$ hearts (data not shown). Interestingly, transgenic mice expressing a PKC-ϵ or PKC-δ translocation inhibitor developed lethal cardiomyopathies (6, 23), highlighting fundamental differences between these mouse models.

Our proteomic analysis demonstrates that several enzymatic isoforms related to glucose metabolism were absent in PKC-$\delta^{-/-}$ hearts. This is in line with a recent report by Caruso et al. (2) suggesting that PKC-δ is required for insulin stimulation of the pyruvate dehydrogenase complex in L6 skeletal muscle cells and immortalized mouse hepatozytes. Pyruvate dehydrogenase catalyzes the oxidation of pyruvate to acetyl-CoA, which represents the irreversible step from glycolysis to the tricarboxylic acid cycle. Altered activitiy of the pyruvate dehydrogenase complex is a likely explanation for the observed changes in glycolytic enzymes in our proteomic analysis.

Interestingly, enzymes related to lipid metabolism, i.e., phosphorylated isoforms of acyl-CoA dehydrogenases, were more abundant in PKC-$\delta^{-/-}$ hearts. To translate such findings into a functional context is a common problem of proteomic analysis because differences at the protein level do not necessarily allow any conclusions about enzymatic activity. In the present study, we demonstrated that NMR analysis is a powerful tool to reveal the metabolic net effect of proteomic changes: the observed decrease in the ratio of glycolytic end products to end products of lipid metabolism suggests that increased fatty acid oxidation might compensate for impaired glycolysis in PKC-$\delta^{-/-}$ hearts, supporting our proteomic findings. Therefore, our study provides the first evidence that loss of PKC-δ is associated with increased lipid metabolism, which would contribute to the inhibition of the pyruvate dehydrogenase complex.

Antioxidants in PKC-$\delta^{-/-}$ hearts. PKC-δ is activated by hydrogen peroxide and has been suggested as a sensor of oxidative stress (8). Our proteomic analysis showed altered expression of antioxidant proteins in PKC-$\delta^{-/-}$ hearts. First, total protein levels and de novo synthesis of 1-Cys prx were decreased in PKC-$\delta^{-/-}$ hearts. This is consistent with a previous report (12) showing that PKC-δ is required for transcriptional activation of peroxiredoxin 1, another member of the peroxiredoxin family. Second, 1-Cys prx was only present in its reduced form in PKC-$\delta^{-/-}$ hearts despite its importance for the detoxification of phospholipid hydroperoxides as well as organic peroxides (derived from short-chain organic fatty acids) (19). This observation is consistent with our previous finding: that loss of PKC-δ is associated with decreased oxidative stress in vascular smooth muscle cells (11). Third, apart from 1-Cys prx, selenium-binding protein 1, which accomplishes the intracellular transport of the trace element (30), was differentially expressed in PKC-$\delta^{-/-}$ hearts. The amino acid selenocysteine is present in various redox enzymes, including the active site of thioredoxin reductase and glutathione peroxidase, which scavenges hydrogen peroxide (7). Thus by modulating the cellular oxidative status, PKC-δ deficiency influences antioxidant expression in murine hearts.

Altered chaperones. Among the PKC- family, PKC-δ and, to a lesser extent, PKC-α, appear to be the most effective HSP kinases (18). Our findings in PKC-$\delta^{-/-}$ mice provide evidence that posttranslational modifications of three chaperones, namely, HSP20, HSP27, and the ζ-subunit of CCT-1, are dependent on PKC-δ. All these chaperones are associated with cytoskeleton function by regulating actin and tubulin polymerization. That PKC-δ activity is required for cytoskeletal integrity has been suggested previously: transgenic mice overexpressing a PKC-δ translocation inhibitor developed myofibril-

lar cardiomyopathy in a dose-dependent fashion, which was characterized by focal cytoskeletal disruption, upregulation of crystalline α/B, and the formation of protein aggregates containing mitochondria (6). Interestingly, small HSPs guard the cytoskeleton from stressful stimuli by phosphorylation-dependent mechanisms and protect cardiomyocytes against oxidative stress (15).

Knockout mice. Recently, we (11) and another group (22) independently developed mice deficient in PKC-δ. Both studies demonstrated that knockout mice developed normally and were fertile. Although PKC-δ is proposed to act as a tumor suppressor, no obvious increase of cancer-induced death was observed. Whereas we observed an abnormal accumulation of vascular smooth muscle cells and accelerated arteriosclerosis in PKC-δ-deficient vein grafts (11), Miyamato et al. (22) showed increased proliferation of B lymphocytes and loss of B cell tolerance in PKC-δ null mice. Given the wide distribution of PKC-δ in cells and tissues, it was rather unexpected that PKC-$\delta^{-/-}$ mice showed a clear phenotype only in certain cells. In the present study, we characterized the metabolic effects of PKC-δ deficiency, which are likely to be relevant for most insulin-sensitive tissues.

In conclusion, we have provided evidence that PKC-δ deficiency is associated with increased lipid metabolism in cardiac tissues. To the best of our knowledge, our study is the first to characterize proteomic as well as metabolomic changes in the same animal model. Our findings could be important for a better understanding of PKC-δ-induced signaling and could lead to new therapeutic strategies for PKC-δ-related diseases.

ACKNOWLEDGMENTS

We thank Dr. M. J. Carden and Dr. A. Roobol (University of Kent, Canterbury, UK) for critical reading of the manuscript and valuable discussion and for providing antibodies to CCT subunits. The use of the facilities of the Medical Biomics Centre at St. George's Hospital Medical School is gratefully acknowledged.

GRANTS

This study was supported by a grant from the Oak Foundation (to Q. Xu).

REFERENCES

1. **Bergmeyer H.** *Methods of Enzymatic Analysis.* Weinheim, Germany: Verlag Chemie, 1974.
2. **Caruso M, Maitan MA, Bifulco G, Miele C, Vigliotta G, Oriente F, Formisano P, and Beguinot F.** Activation and mitochondrial translocation of protein kinase Cdelta are necessary for insulin stimulation of pyruvate dehydrogenase complex activity in muscle and liver cells. *J Biol Chem* 276: 45088–45097, 2001.
3. **Chen L, Hahn H, Wu G, Chen CH, Liron T, Schechtman D, Cavallaro G, Banci L, Guo Y, Bolli R, Dorn GW Jr, and Mochly-Rosen D.** Opposing cardioprotective actions and parallel hypertrophic effects of delta PKC and epsilon PKC. *Proc Natl Acad Sci USA* 98: 11114–11119, 2001.
4. **Dunn MJ.** Two-dimensional polyacrylamide gel electrophoresis for the separation of proteins for chemical characterization. *Methods Mol Biol* 64: 25–36, 1997.
5. **Fan TW, Higashi RM, Lane AN, and Jardetzky O.** Combined use of ^{1}H-NMR and GC-MS for metabolite monitoring and in vivo ^{1}H-NMR assignments. *Biochim Biophys Acta* 882: 154–167, 1986.
6. **Hahn HS, Yussman MG, Toyokawa T, Marreez Y, Barrett TJ, Hilty KC, Osinska H, Robbins J, and Dorn GW Jr.** Ischemic protection and myofibrillar cardiomyopathy: dose-dependent effects of in vivo deltaPKC inhibition. *Circ Res* 91: 741–748, 2002.
7. **Holmgren A.** Antioxidant function of thioredoxin and glutaredoxin systems. *Antioxid Redox Signal* 2: 811–820, 2000.
8. **Huang HC, Nguyen T, and Pickett CB.** Phosphorylation of Nrf2 at Ser-40 by protein kinase C regulates antioxidant response element-mediated transcription. *J Biol Chem* 277: 42769–42774, 2002.
9. **Inagaki K, Hahn HS, Dorn GW Jr, and Mochly-Rosen D.** Additive protection of the ischemic heart ex vivo by combined treatment with δ-protein kinase C inhibitor and ϵ-protein kinase C activator. *Circulation* 108: 869–875, 2003.
10. **Kikkawa U, Matsuzaki H, and Yamamoto T.** Protein kinase Cdelta (PKCdelta): activation mechanisms and functions. *J Biochem (Tokyo)* 132: 831–839, 2002.
11. **Leitges M, Mayr M, Braun U, Mayr U, Li C, Pfister G, Ghaffari-Tabrizi N, Baier G, Hu Y, and Xu Q.** Exacerbated vein graft arteriosclerosis in protein kinase Cdelta-null mice. *J Clin Invest* 108: 1505–1512, 2001.
12. **Li B, Ishii T, Tan CP, Soh JW, and Goff SP.** Pathways of induction of peroxiredoxin I expression in osteoblasts: roles of p38 mitogen-activated protein kinase and protein kinase C. *J Biol Chem* 277: 12418–12422, 2002.
13. **Li C, Hu Y, Mayr M, and Xu Q.** Cyclic strain stress-induced mitogen-activated protein kinase (MAPK) phosphatase 1 expression in vascular smooth muscle cells is regulated by Ras/Rac-MAPK pathways. *J Biol Chem* 274: 25273–25280, 1999.
14. **Li C, Hu Y, Sturm G, Wick G, and Xu Q.** Ras/Rac-dependent activation of p38 mitogen-activated protein kinases in smooth muscle cells stimulated by cyclic strain stress. *Arterioscler Thromb Vasc Biol* 20: E1–E9, 2000.
15. **Liang P and MacRae TH.** Molecular chaperones and the cytoskeleton. *J Cell Sci* 110: 1431–1440, 1997.
16. **Liu H, McPherson BC, and Yao Z.** Preconditioning attenuates apoptosis and necrosis: role of protein kinase C-ϵ and -δ isoforms. *Am J Physiol Heart Circ Physiol* 281: H404–H410, 2001.
17. **Llorca O, Martin-Benito J, Ritco-Vonsovici M, Grantham J, Hynes GM, Willison KR, Carrascosa JL, and Valpuesta JM.** Eukaryotic chaperonin CCT stabilizes actin and tubulin folding intermediates in open quasi-native conformations. *EMBO J* 19: 5971–5979, 2000.
18. **Maizels ET, Peters CA, Kline M, Cutler RE Jr, Shanmugam M, and Hunzicker-Dunn M.** Heat-shock protein-25/27 phosphorylation by the delta isoform of protein kinase C. *Biochem J* 332: 703–712, 1998.
19. **Manevich Y, Sweitzer T, Pak JH, Feinstein SI, Muzykantov V, and Fisher AB.** 1-Cys peroxiredoxin overexpression protects cells against phospholipid peroxidation-mediated membrane damage. *Proc Natl Acad Sci USA* 99: 11599–11604, 2002.
20. **Mayr M, Metzler B, Chung YL, McGregor E, Mayr U, Troy H, Hu Y, Leitges M, Pachinger O, Griffiths JR, Dunn MJ, and Xu Q.** Ischemic preconditioning exaggerates cardiac damage in PKC-δ null mice. *Am J Physiol Heart Circ Physiol*: H946–H956, 2004.
21. **McGregor E, Kempster L, Wait R, Welson SY, Gosling M, Dunn MJ, and Powel JT.** Identification and mapping of human saphenous vein medial smooth muscle proteins by two-dimensional polyacrylamide gel electrophoresis. *Proteomics* 1: 1405–1414, 2001.
22. **Miyamoto A, Nakayama K, Imaki H, Hirose S, Jiang Y, Abe M, Tsukiyama T, Nagahama H, Ohno S, Hatakeyama S, and Nakayama KI.** Increased proliferation of B cells and auto-immunity in mice lacking protein kinase Cdelta. *Nature* 416: 865–869, 2002.
23. **Mochly-Rosen D, Wu G, Hahn H, Osinska H, Liron T, Lorenz JN, Yatani A, Robbins J, and Dorn GW Jr.** Cardiotrophic effects of protein kinase C epsilon: analysis by in vivo modulation of PKCepsilon translocation. *Circ Res* 86: 1173–1179, 2000.
24. **Munz B, Frank S, Hubner G, Olsen E, and Werner S.** A novel type of glutathione peroxidase: expression and regulation during wound repair. *Biochem J* 326: 579–585, 1997.
25. **Naruse KK, GL.** Protein kinase C and myocardial biology and function. *Circ Res* 86: 1104–1106, 2000.
26. **Ohmori S, Shirai Y, Sakai N, Fujii M, Konishi H, Kikkawa U, and Saito N.** Three distinct mechanisms for translocation and activation of the delta subspecies of protein kinase C. *Mol Cell Biol* 18: 5263–5271, 1998.
27. **Perkins DN, Pappin DJ, Creasy DM, and Cottrell JS.** Probability-based protein identification by searching sequence databases using mass spectrometry data. *Electrophoresis* 20: 3551–3567, 1999.
28. **Rabilloud T, Heller M, Gasnier F, Luche S, Rey C, Aebersold R, Benahmed M, Louisot P, and Lunardi J.** Proteomics analysis of cellular response to oxidative stress. Evidence for in vivo overoxidation of peroxiredoxins at their active site. *J Biol Chem* 277: 19396–19401, 2002.

29. **Rybin VO, Sabri A, Short J, Braz JC, Molkentin JD, and Steinberg SF.** Cross-regulation of novel protein kinase C (PKC) isoform function in cardiomyocytes. Role of PKC epsilon in activation loop phosphorylations and PKC delta in hydrophobic motif phosphorylations. *J Biol Chem* 278: 14555–14564, 2003.
30. **Sani BP, Woodard JL, Pierson MC, and Allen RD.** Specific binding proteins for selenium in rat tissues. *Carcinogenesis* 9: 277–284, 1988.
31. **Shevchenko A, Wilm M, Vorm O, and Mann M.** Mass spectrometric sequencing of proteins silver-stained polyacrylamide gels. *Anal Chem* 68: 850–858, 1996.
32. **Soltoff SP.** Rottlerin is a mitochondrial uncoupler that decreases cellular ATP levels and indirectly blocks protein kinase Cdelta tyrosine phosphorylation. *J Biol Chem* 276: 37986–37992, 2001.
33. **Wagner E, Luche S, Penna L, Chevallet M, Van Dorsselaer A, Leize-Wagner E, and Rabilloud T.** A method for detection of overoxidation of cysteines: peroxiredoxins are oxidized in vivo at the active-site cysteine during oxidative stress. *Biochem J* 366: 777–785, 2002.
34. **Xu Q, Li DG, Holbrook NJ, and Udelsman R.** Acute hypertension induces heat-shock protein 70 gene expression in rat aorta. *Circulation* 92: 1223–1229, 1995.
35. **Yan JX, Wait R, Berkelman T, Harry RA, Westbrook JA, Wheeler CH, and Dunn MJ.** A modified silver staining protocol for visualization of proteins compatible with matrix-assisted laser desorption/ionization and electrospray ionization-mass spectrometry. *Electrophoresis* 21: 3666–3672, 2000.